Research in Pharmaceutical Sciences, December 2017; 12(6): 465-478
Received: October 2016
Accepted: September 2017

School of Pharmacy & Pharmaceutical Sciences
Isfahan University of Medical Sciences

Original Article

Preparation and *in vitro* characterization of retinoic acid-loaded poly(ε-caprolactone)-poly(ethylene glycol)-poly(ε-caprolactone) micelles

Ebrahim Shakiba[1], Saeedeh Khazaei[2], Marziyeh Hajialyani[3], Bandar Astinchap[4], and Ali Fattahi[5,*]

[1]*Department of Biochemistry, School of Medicine, Kermanshah University of Medical Sciences, Kermanshah, I.R. Iran.*
[2]*Department of Pharmaceutics, School of Pharmacy, Kermanshah University of Medical Sciences, Kermanshah, I.R. Iran.*
[3]*Pharmacutical Sciences Research Center, Faculty of Pharmacy, Kermanshah University of Medical Sciences, Kermanshah, I.R. Iran.*
[4]*Department of Physics, Faculty of Science, Kurdistan University, Sanandaj, I.R. Iran.*
[5]*Nano Drug Delivery Research Center, Kermanshah University of Medical Sciences, Kermanshah, I.R. Iran.*

Abstract

In order to achieve the controlled release of all-trans-retinoic acid (ATRA), poly(ε-caprolactone)-poly(ethylene glycol)-poly(ε-caprolactone) (PCL-PEG-PCL) copolymer with average molecular weight of 5.34 kDa was synthesized. The nanosized micelles were prepared from copolymer by nano-precipitation method. Critical association concentration (CAC) of micelles was measured by fluorimetry and results indicated low CAC value of micelles (1.9×10^{-3} g/L). ATRA was encapsulated in the core of micelles using different ratios of drug to copolymer. In the case of 10% drug to polymer ratio, more than 80% of the drug was released within 3 days, whereas for ratio of 2% more than 90% of the drug was released within 3 h. The cytotoxic study performed by MTT assay showed that H1299 survival percent decreased significantly ($P \leq 0.05$) after exposure to drug-loaded micelles, while no proliferation inhibition effect was observed by either free ATRA or blank PCL-PEG-PCL micelles.

Keywords: Poly(ε-caprolactone)-poly(ethylene glycol)-poly(ε-caprolactone); Micelle; All trans retinoic acid (ATRA); H1299; Cytotoxicity

INTRODUCTION

All-trans-retinoic acid (ATRA) is now being widely distributed for the treatment of many proliferative diseases because of its anticancer properties and its advantages in the chemoprevention, treatment of cancer, and cell and tissue engineering (1-3). Specially, it has been used for patients with acute myelogenous leukemia (AML) to induce remission in patients (4). Furthermore, ATRA can inhibit the growth and squamous differentiation of the bronchial epithelial cells (5). Several studies reported the efficacy of ATRA in patients with metastatic non-small cell lung cancer (NSCLC) (6,7).

ATRA showed potential for increasing the response rate and progression free survival for the patients with NSCLC with an acceptable toxicity profile (8). ATRA can inhibit the proliferation, induce markers of apoptosis and squamous differentiation, and prevent the process of cell migration induced by ATRA in NSCLC (9,10).

The ATRA mechanism of action in cancer therapy could be mainly attributed to its binding to retinoic acid receptors or retinoid X receptors in the nuclear membrane of cancer cells, which causes inducing growth inhibition, differentiation, or apoptosis in the cancer cells (11). Despite its advantages, it suffers from some drawbacks such as drug resistance, hyper-triglyceridemia, mucocutaneous dryness, and headache (12).

*Corresponding author: A. Fattahi
Tel: +98-8334276489, Fax: +98-8334276493
Email: a.fatahi.a@gmail.com

Access this article online

Website: http://rps.mui.ac.ir

DOI: 10.4103/1735-5362. 217427

Furthermore, in the case of oral administration, a RA-inducible P-450 cytochrome called p450AI metabolizes it in the liver, and its concentration in systemic circulation decreases gradually (13). In order to overcome the instability drawbacks and improve the therapeutic efficacy, parenteral administration could be used as one of the most useful strategies. One of the complications during parenteral treatment with ATRA is the poor water solubility of this agent (14). It is also decomposed or exchanged to the isotretinoin as an isomerized product or to the all-trans-4-oxo as an oxidized product by exposing to various factors such as light, heat, and oxidants (15,16). In order to overcome such drawbacks, researchers have tried to develop an I.V. injectable formulation of ATRA, using different bioactive drug carriers such as cyclodextrins, liposomes, micelles, and micro-emulsions (17-21).

Polymeric micelles possess a core-shell structure containing hydrophobic segments as internal core surrounding by hydrophilic segments, as a shell in an aqueous medium. They have advantages compared to low molecular weight surfactant micelles, because they have lower critical association concentration (CAC) and are more stable in aqueous media (22,23). Among the compounds used widely in drug delivery, poly(ε-caprolactone) (PCL) is regarded as a promising candidate for biomedical applications due to its advantages such as biocompatibility and biodegradability, and non-toxicity toward living organisms (24). Despite its advantages, it suffers from some drawbacks such as great hydrophobicity and slow biodegradation rate which limited its efficacy in biomedicine. Poly (ethylene glycol) (PEG) has been used on the outer surface of polymeric micelles, due to its beneficial characteristics of pharmacokinetic of the micelles; i.e., long-circulating characteristics and significant tumor accumulation. Considering its properties such as nontoxicity, hydrophilicity, solubility in water and organic solvents, and absence of antigenicity and immunogenicity, PEG could be used for many clinical applications (25,26). It has been found that PEG can form a hydrated steric barrier which prevents micelles from protein absorption, cell adhesion, recognition, and sequestration by the body's defense system.

In the present study, hydrophilic PEG was incorporated into the main chain of PCL to obtain an amphiphilic triblock PCL-PEG-PCL copolymer. PCL-PEG-PCL is a thermo-sensitive copolymer which is more flexible than PCL-PEG diblock copolymer for drug loading and drug delivery (23). Also, the micelles produced by triblock copolymers are more stable and have lower CAC than the diblock copolymer micelles (27,28) which make PCL-PEG-PCL triblock copolymer more advantageous than PCL-PEG copolymer for the micellar drug delivery systems. ATRA, a hydrophobic anticancer drug, was incorporated into the PCL-PEG-PCL amphiphilic copolymer and physicochemical analyses such as ^{1}H NMR spectroscopy, atomic-force microscopy (AFM), XRD, particle size, zeta potential, FTIR, and *in vitro* cytotoxicity were performed.

MATERIALS AND METHODS

Materials

ε-caprolactone (ε-CL), ATRA, stannous octoate ($Sn(Oct)_2$), dimethyl sulfoxide (DMSO), and nile red were purchased from Sigma Aldrich (USA) and were used without any purification. Poly(ethylene glycol) (PEG, Mn, 1500) was purchased from Merck (Germany). Dialysis membrane (molecular weight cutoff 3500) was purchased from Orange scientific (USA).

Synthesis of PCL-PEG-PCL and preparation of PCL-PEG-PCL micelles

The PCL-PEG-PCL copolymer was prepared by ring-opening polymerization of ε-CL initiated by PEG. 0.1 g (0.0087 mol) of ε-CL, 0.5 g (0.0003 mol) of PEG 1500, and 0.005 g of $Sn(Oct)_2$ added into three-necked vessel under vacuum, then the reaction system was kept at 130 ºC for 6 h. After degassing under vacuum for another 30 min, the resultant copolymer was cooled to room temperature and precipitated in excess cold diethyl ether (29). The synthesis was approved by FTIR and ^{1}H NMR spectroscopy.

PCL-PEG-PCL blank nanomicelles were fabricated with nanoprecipitation method, and polymers were dissolved in acetone as the organic solvent (30).

^{1}H NMR analysis

^{1}H NMR spectra (in CDCl3) were recorded on ultra-shield 400 spectrometer (Bruker, Germany) at 400 MHz and tetramethylsilane was utilized as an internal reference standard.

FTIR analysis

The FTIR spectra of PCL-PEG-PCL copolymer, blank, and drug-loaded micelles were observed using FTIR spectrometer (IR prestige-21, Shimadzu, Japan), in the spectral range of 4000-400 cm^{-1} at a resolution of 4 cm^{-1}.

Molecular weight analysis

The ^{1}H NMR spectrum of PCL-PEG-PCL was used to calculate the number average molecular weight (Mn) and the ratio of PCL/PEG of the copolymer. These properties were calculated using following equations:

$$2(2(x-1)) / I_a = 4 / I_d \quad (1)$$

$$(4(y-2) + 4) / I_f = 4 / I_d \quad (2)$$

$$M_{n\ (PCL\text{-}PEG\text{-}PCL)} = M_{n\ (PEG)} + M_{n\ (PCL)} = 44y + 2(114x) \quad (3)$$

where, I_a, I_d, and I_f were integral intensities of methylene protons of $-CH_2OOC-$ in PCL units at 4.06 ppm, methylene protons of $-O-CH_2-$ in PEG end unit at 4.23 ppm, and methylene hydrogen of homo-sequences of PEG units at 3.65 ppm, respectively (Fig. 1). X and y were respectively the corresponding block number of PCL and PEG in PCL-PEG-PCL copolymer (29).

The molecular weight of the copolymer was also measured by static light scattering (SLS) technique using Zetasizer (Zetasizer-ZEN3600 Malvern Instrument Ltd., Worcestershire, UK). The average scattering intensity from seven different concentrations of the PCL-PEG-PCL copolymer (3-35 mg/mL) were recorded using the Malvern supplied 'molecular weight' operating procedure. The instrument measured molecular weight using Rayleigh equation and Debye Plot. The solvent of the polymer (toluene) was used as the standard reference (31).

Preparation and characterization of ATRA-loaded PCL-PEG-PCL micelles

The method for preparing the ATRA loaded nanomicelles was completely similar to aforementioned method for preparing blank PCL-PEG-PCL nanomicelles. Briefly, different solutions with constant weights of PCL-PEG-PCL and different amounts of ATRA in acetone were prepared to form an organic phase. Then, the organic phase was added dropwise to distilled water and stirred magnetically at room temperature. At this step, acetone started to diffuse into distilled water and amphiphilic PCL-PEG-PCL block copolymer self-assembled into nanomicelles. ATRA was encapsulated in the hydrophobic core of copolymer in aqueous solution.

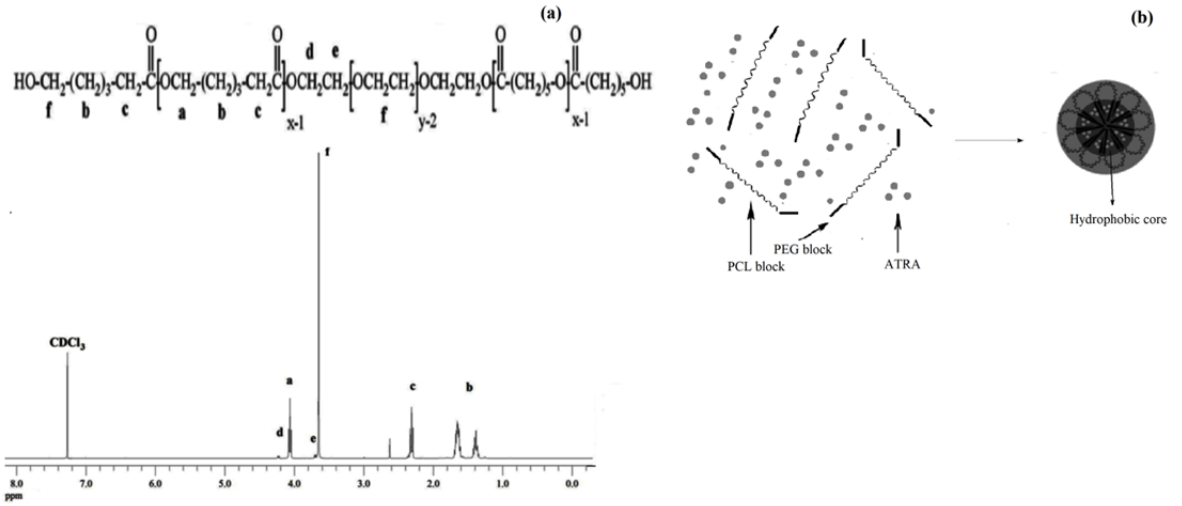

Fig. 1. (a) ^{1}H NMR spectrum of PCL-PEG-PCL and (b) orientation of the polymer in micelles structure.

The loading efficiency was assessed at different ratios of ATRA to copolymer (1, 2, 5, 10, and 20%). The obtained suspension was filtered by 400 nm syringe filter to remove unloaded insoluble ATRA (32). In order to determine the loading efficiency, 200 µL of the drug-loaded micelle solution was added to 1000 µL DMSO and was vortexed for 1 min to break down the micelles. The absorbance was measured using a UV-Vis spectrophotometer (UV mini-1240, Shimadzu, Japan) at the wavelength of 360 nm. The standard curve of ATRA was prepared at different concentrations in a mixture of DMSO and water with 1:5 DMSO to water volume ratio. Drug content (DC) and loading efficacy (LE) were calculated by equations 4 and 5:

$$LE = \frac{\text{Weight of the drug in nanoparticles}}{\text{Weight of the feeding drugs}} \times 100 \quad (4)$$

$$DC = \frac{\text{Weight of the drug in nanoparticles}}{\text{Weight of the drug in nanoparticles + Weight of the copolymers used}} \times 100 \quad (5)$$

Physicochemical characterization of PCL-PEG-PCL and drug-loaded micelles

CAC of PCL-PEG-PCL micelles

The CAC was measured using fluorescence measurements, and nile red (3.2×10^{-7} M) was utilized as the probe. Excitation of the hydrophobic nile red with 490 nm light in an aqueous medium results in a relatively low fluorescence with a λ_{max} of 540 nm. However, if it resides in a hydrophobic environment, such as the core of a micelle, its fluorescence emission intensity increases significantly and experiences a blue shift to 520 nm. The emission spectrum of various polymer concentrations (5×10^{-4} to 0.5 g/L) was recorded using fluorescence spectrometer (LS45, Perkin Elmer, USA). The fluorescence emission of solutions was determined at a wavelength of 520 nm, and the emission of nile red in the absence of copolymer was determined at a wavelength of 540 nm (excitation and emission wavelengths: 490 and 500-650 nm, respectively).

Particle size and zeta potential measurements

The particle size, polydispersity index (PDI), and zeta potential of the prepared blank and drug-loaded micelles were measured using Zetasizer with dynamic light scattering (DLS) technique. The zeta potential of nanomicelles was determined from their electrophoretic mobility using Henry equation.

Morphological studies

A complementary morphological analysis was conducted using AFM (Nanosurf® Mobile S., Switzerland) in the non-contact mode. PCL-PEG-PCL micelle was placed on a washed mica slide and was dried at room temperature before morphology analysis.

Crystallographic assays

XRD (EQUINOX 3000, Inel, France) was performed to prepare crystallographic assays on ATRA powder, blank PCL-PEG-PCL nanomicelles, and ATRA loaded PCL-PEG-PCL nanomicelles. Samples were in the solid form for XRD analysis. The applied voltage and current were 30 kV and 20 mA, using Cu Kα radiation.

In vitro drug release study

To determine the *in vitro* release kinetics of ATRA from nanomicelles, 0.5 mL of ATRA-loaded PCL-PEG-PCL nanomicelles was placed into a dialysis bag (cut off 3500 Da). The dialysis bags were incubated in 25 mL of phosphate-buffer saline (PBS, pH 7.4) containing 2% ethanol at 37 °C under gentle shaking, and 1 mL of incubation medium was replenished by the fresh medium at specific time intervals. The amount of ATRA in release medium after time intervals was determined using UV spectrophotometry at 360 nm.

The standard curve of ATRA in PBS (containing 2% ethanol) was prepared and the cumulative release profile was demonstrated versus time.

In the release study, sink condition was provided and the volume of release medium was adjusted in a way that ATRA never was saturated in the medium (considering 3 mg/L of maximum solubility of ATRA in water), and 2% ethanol was used to improve solubility of ATRA. This procedure was repeated trice and results were expressed as the mean value ± SD.

Cell culture

H1299 (human non-small lung carcinoma) cell line was purchased from the Pasteur Institute of Iran. Cells were maintained in the RPMI-1640 supplemented with 10% (v/v) fetal bovine serum (FBS) and penicillin/streptomycin (50 IU ml^{-1}, 50 µg ml^{-1}) at 37 ºC in a humidified atmosphere containing 5% CO2. Cells were sub-cultured regularly using trypsin/EDTA.

In vitro proliferation assay

The *in vitro* viability of H1299 cells was assessed using MTT test. Specifically, the H1299 cells were seeded in the 96-well plates and grown for 24 h. The cells were added to wells with different concentrations of the blank micelle, free ATRA, and ATRA-loaded micelles at 37 ºC and incubated for another 48 h. At the end of the incubation period, 20 mL of MTT solution at concentration of 5 mg/mL was added and incubated for 3 h at 37 ºC. Each well was then washed with 50 mL of PBS. Then, 150 mL of DMSO was added to each well to dissolve the formazan crystals. Finally, the absorbance was recorded using ELISA plate reader (Bio-Rad, Model 680, USA). The test and the reference wavelengths were 570 and 630 nm, and the sample signal was determined (OD570-OD630) (33). All the experiments were performed in triplicate.

RESULTS

Synthesis of PCL-PEG-PCL and preparation of drug-loaded micelles

The amphiphilic PCL-PEG-PCL copolymers were synthesized via the ring-opening copolymerization in the absence of toxic catalyst or initiator. It should be noted that for these types of copolymers, both ends of the PEG blocks are anchored at the core/shell interfaces, and the loops should be formed at the surface of the micelles by PEG chains. This molecular orientation is different from that for the micelles of the diblock copolymer. In the diblock copolymer, only one end of the PEG block should be anchored at the core/shell interface, and PEG chains form the brush-like structures at the surface of the micelles (34). The orientation of polymers in the copolymer and ^1H NMR spectrum of the obtained PCL-PEG-PCL copolymer is shown in Fig. 1. The presence of a sharp peak at 3.65 ppm could be related to the methylene protons of $-CH_2CH_2O-$ in the PEG units of the triblock copolymer. Two weak peaks at 4.23 and 3.82 ppm could be assigned to the methylene protons of $-O-CH_2-CH_2-$ at the end unit of PEG linked to PCL-PEG-PCL blocks. The presence of two characteristic peaks at 1.40 and 1.65 ppm could be related to the methylene protons of $-(CH_2)_3-$, and the peak at 2.32 ppm is attributed to the methylene proton of $-OCCH_2-$ in PCL units of the triblock copolymer.

The peak at 4.06 ppm could be related to $-CH_2OOC-$ in PCL units, and the peak at 2.62 ppm is assigned to the proton of OH at the end of PCL units in the copolymer. The observed peaks in the range of 1.4 - 2.5 ppm, which could be related to aliphatic protons of $-(CH_2)_3-$ and $-OCCH_2-$ in PCL units and the peaks in the range of 3.5 - 4.5 ppm, which could be related to $-OCH_2$ confirmed the synthesis of the copolymer. ^1H NMR spectrum was also used to estimate M_n and PCL/PEG block ratio, which were 5.26 kDa and 3.15, respectively. The drug-encapsulated micelles were prepared by nanoprecipitation method and then lyophilized to turn them into powder.

FTIR spectroscopy results

The FTIR spectrum of the synthesized PCL-PEG-PCL is shown in Fig. 2a. The absorption band at 1728 cm^{-1} is assigned to the C=O stretching vibrations of the ester carbonyl group. The absorption bands at 1107 and 1242 cm^{-1} are attributed to the C-O-C stretching vibrations of the repeated $-OCH_2CH_2$ units of PEG, and the C-O stretching vibrations, respectively. The absorption band at 3433 cm^{-1} is attributed to the terminal hydroxyl groups (-OH) in the copolymer. According to physical mixture spectrum of caprolactone/PEG (Fig. 2b), the absorption band at 1732 cm^{-1} was attributed to the C=O stretching vibrations of caprolactone, and there was no absorption band at 1728 cm^{-1} assigned to the C=O of the ester carbonyl group of PCL-PEG-PCL which approved synthesis of the copolymer.

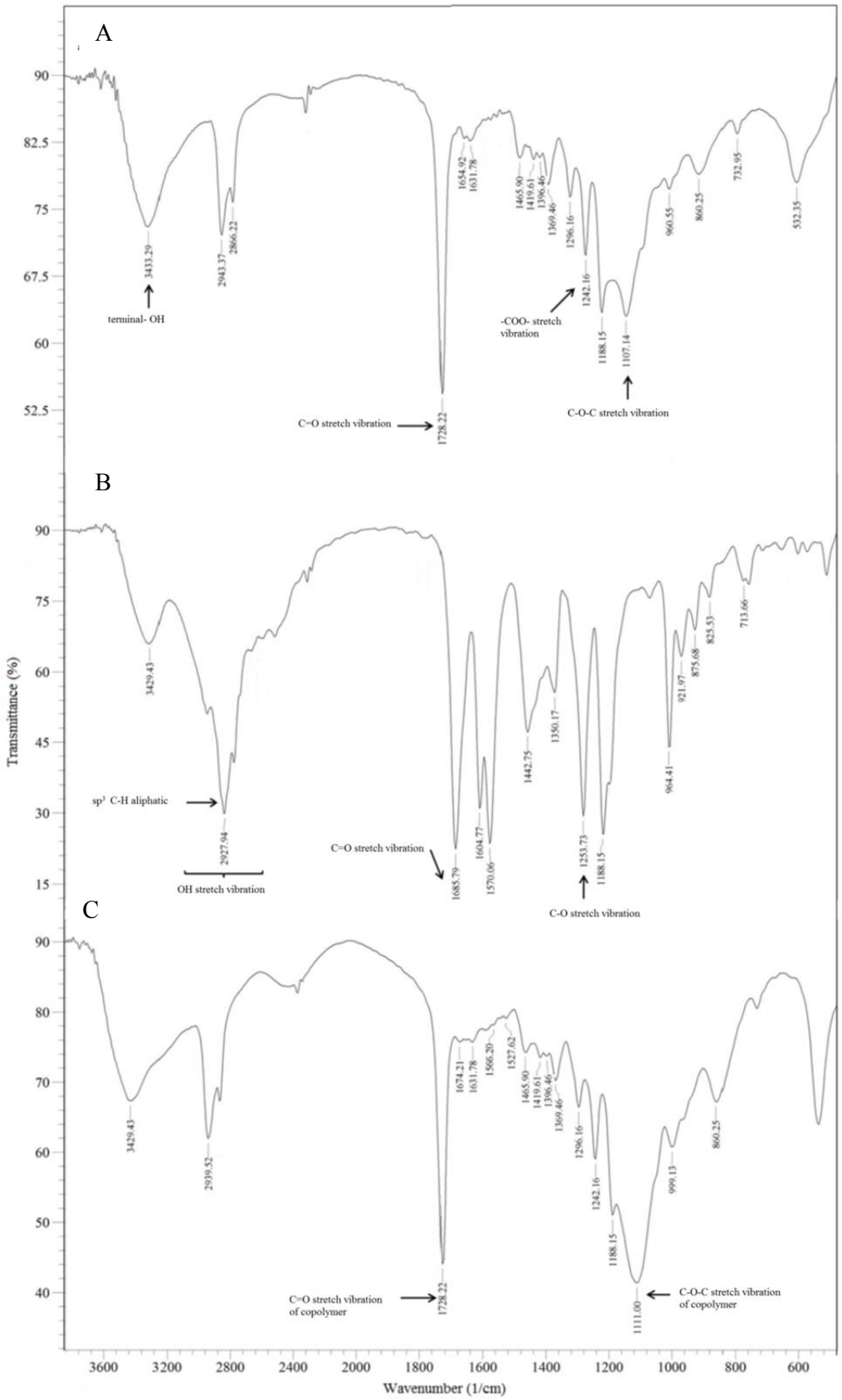

Fig. 2. FTIR spectra of (A), PCL-PEG-PCL; (B), ATRA; and (C), ATRA loaded PCL-PEG-PCL micelles (feeding ratio of 10%).

In the spectrum of ATRA (Fig. 2c), the characteristic peaks at 1685 and 1253 cm^{-1} are assigned to the C=O of carboxylic group. The peak in the range of 2600-3429 cm^{-1} is attributed to the OH functional group of carboxylic acid, and the peak at 2928 cm^{-1} is attributed to the C-H of double bonds of ATRA. In the spectrum of ATRA-loaded micelles, the presence of peaks at 1111, 1728, and 2993 cm^{-1} could be assigned to the vibrations of C-O, C=O (ester carbonyl group), and C-H of double bonds. The peaks at 1674, 1566, and 999 cm^{-1} in drug loaded micelles (feeding ratio of 10%) spectrum are attributed to ATRA. (Fig.2d).

Physicochemical properties of PCL-PEG-PCL micelles

In the aqueous mediums, the hydrophobic PCL moieties of the PCL-PEG-PCL could be assembled spontaneously in hydrophobic cores, surrounding by hydrophilic PEG backbones. The dye solubilization method was performed to assess spontaneous self-assembling of the PCL-PEG-PCL in the aqueous solvent using nile red. After formation of micelles in an aqueous medium, nile red shows tendency to penetrate inside the hydrophobic core. Since nile red is poorly soluble in water, it shows large tendency to penetrate into the micelles or other aggregates. Fig. 3 shows the variation of the fluorescence intensity versus the logarithm of the concentration of PCL-PEG-PCL micelles.

The CAC values were defined as the crossover point of the two straight lines in the curve (Fig. 3) (35). There are no significant changes in the intensities of concentrations lower than the CAC, whereas, in concentrations higher than the CAC, a linear increase in the intensities was observed with increasing the concentration of PCL-PEG-PCL micelles. The CAC of the PCL-PEG-PCL micelles was 1.9×10^{-3} g/L. The data of particle size, polydispersity, and zeta potential of blank micelles are summarized in Table 1.

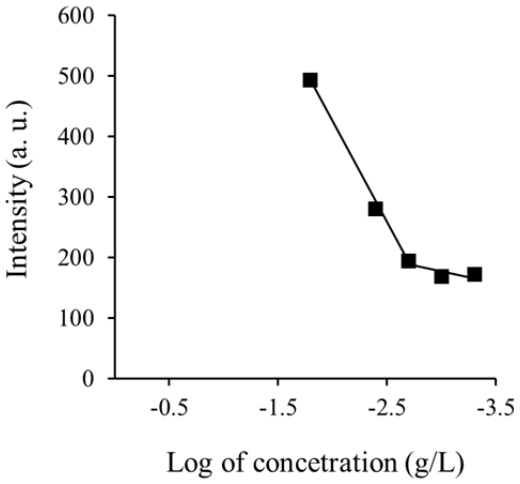

Fig. 3. Plots of the Intensity of nile red emission peak at 520 nm (excitation and emission wavelengths: 480 and 500-650 nm, respectively) versus logarithm concentration of nanomicelles.

Table 1. Size, PDI, and zeta potential of nanomicelles at different feeding ratios and their loading efficiency and drug content.

Sample name	Size (nm)	PDI	Zeta (mV)	LE (w/w %)	DC (w/w %)
Blank particle	147.95 ± 3.04	0.14 ± 0.04	-15.06 ± 1.65		
Feeding ratio (1%)	124.05 ± 0.35	0.06 ± 0.01	-15.20 ± 3.25	35.37 ± 5.25	0.35 ± 0.05
Feeding ratio (2%)	134.80 ± 1.27	0.26 ± 0.03	-22.93 ± 5.31	34.06 ± 12.30	0.67 ± 0.24
Feeding ratio (5%)	162.10 ± 11.17	0.47 ± 0.01	-24.90 ± 2.34	24.59 ± 3.63	1.21 ± 0.17
Feeding ratio (10%)	288.75 ± 0.64	0.57 ± 0.22	-30.40 ± 1.15	25.73 ± 3.70	2.51 ± 0.35
Feeding ratio (20%)	195.95 ± 34.71	0.36 ± 0.14	-30.03 ± 3.42	14.19 ± 1.11	2.76 ± 0.21

PDI, polydispersity index; LE, loading efficiency, and DC, drug content.

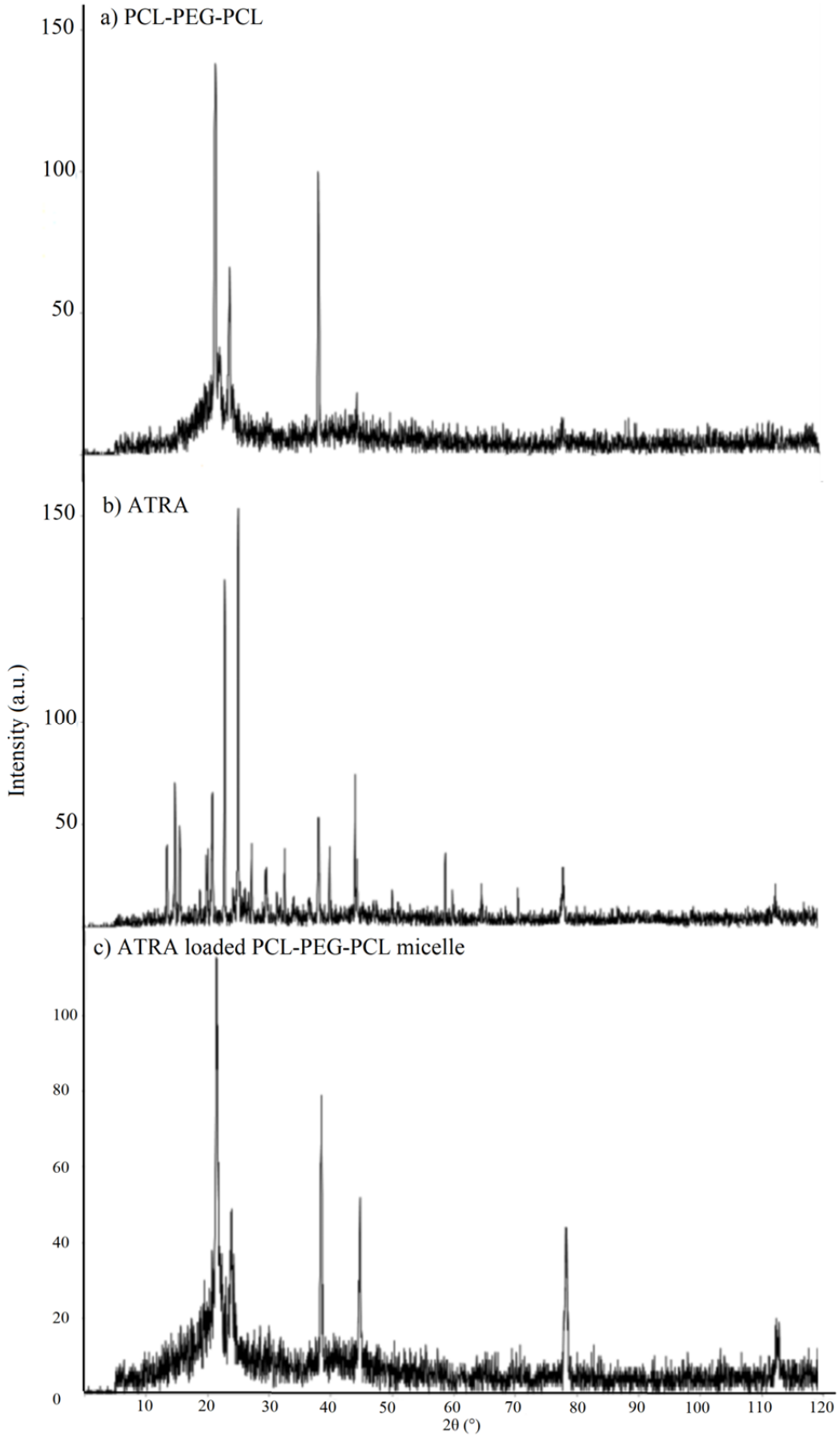

Fig. 4. XRD pattern of (a) PCL-PEG-PCL, (b) ATRA, and (c) ATRA loaded PCL-PEG-PCL micelles (feeding ratio of 10%).

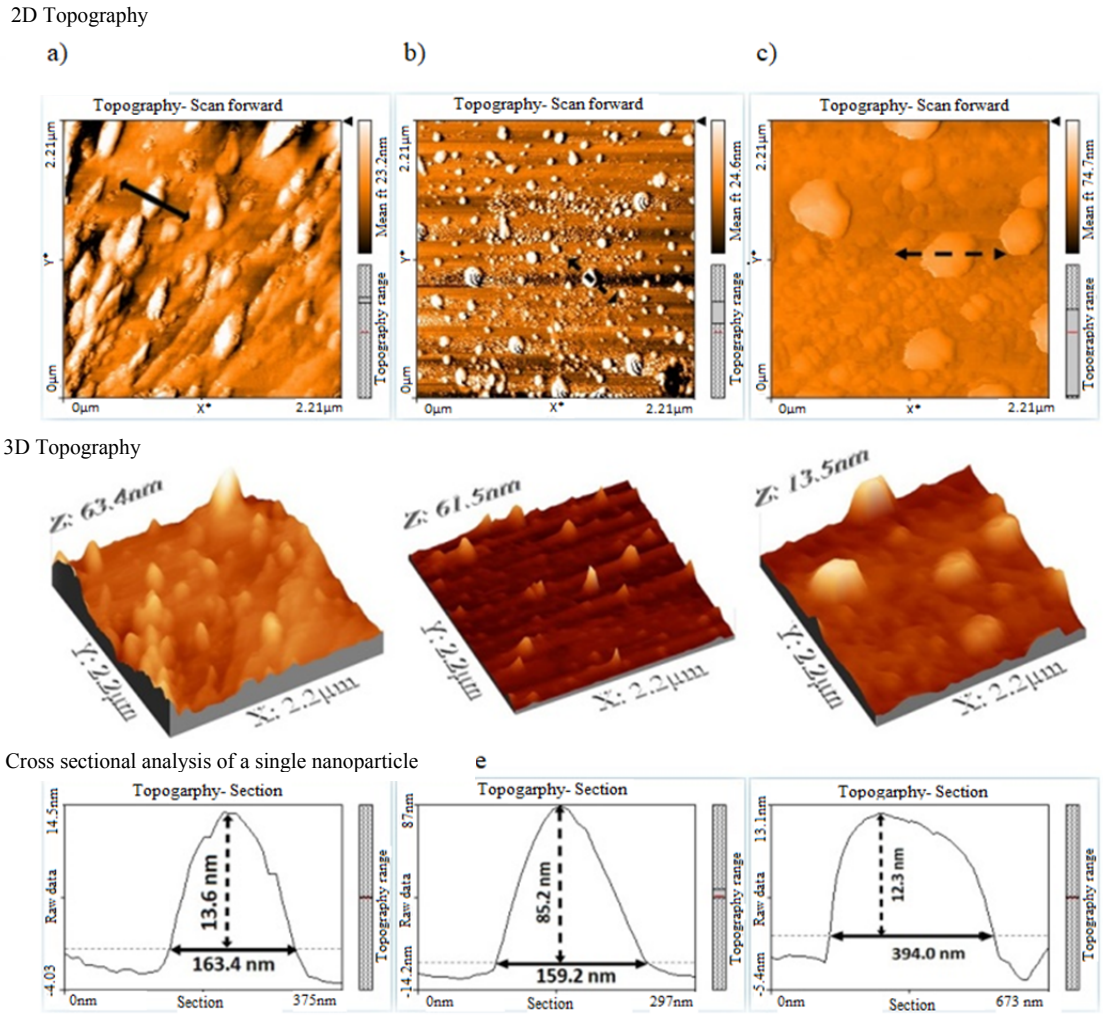

Fig. 5. AFM image of nanomicelles: (a) blank PCL–PEG–PCL nanomicelles, (b) ATRA loaded PCL-PEG-PCL micelles (feeding ratio of 2%), and (c) ATRA loaded PCL-PEG-PCL micelles (feeding ratio of 10%). The graphs in bottom indicate profile of the cross-section along the arrow in 2D topography.

XRD crystallographic results

Crystallographic studies were performed on ATRA, blank nanomicelles, and ATRA-loaded nanomicelles as presented in Fig. 4. The X-ray spectrum of PCL-PEG-PCL is illustrated in Fig. 4a. ATRA The powder X-ray diffraction pattern of pure ATRA confirmed the crystalline state of the drug (Fig. 4b). Three crystalline diffraction peaks, corresponding to ATRA, were observed at the diffraction angles (2θ) of 44, 78, and 112 ° in the diffractogram of ATRA-loaded PCL-PEG-PCL nanomicelles. (Fig. 4c).

LE, DC, particle size, PDI, and zeta potential of the nanomicelles before and after loading are summarized in Table 1. An increase in feeding ratio (weight ratio of ATRA/PCL-PEG-PCL) caused decreasing the LE and increasing the DC. These results are in agreement with the results obtained in similar studies carried out for loading of hydrophobic drugs into the micelles (35).

Morphology of the micelles

The morphology of nanomicelles was investigated by AFM. Fig. 5 shows the AFM images of nanomicelles in non-contact and dynamic force operating modes. A glance at Figs. 5a to 5c indicates that ATRA-loaded micelles are more spherical than blank micelles. The length and width of the fusiform blank micelles, obtained by AFM, were found 143 and 309 nm, respectively; whereas, the average size of micelles was about 150 nm for feeding ratio of 2% and 304 nm for feeding ratio of 10%, which is in good agreement with DLS data. The size obtained by AFM was bigger than that obtained by DLS.

In vitro drug release from PCL-PEG-PCL micelles

The release percentage of ATRA from nanomicelles was calculated and the results are illustrated in Fig. 6. The results showed that for feeding ratio of 10%, more than 80% of the ATRA was released during three days, whereas for feeding ratio of 2% more than 90% of ATRA was released within 3 h.

In vitro cytotoxicity

The *in vitro* viability of H1299 cells at 48 h are shown in Fig. 7. We have investigated the viability of these cells in the presence of micelles with the drug to polymer ratio of 2% and 10%, and free ATRA (the amount of free ATRA was similar to that in the ATRA loaded PCL-PEG-PCL nanomicelles). ATRA is known to inhibit mitosis and the proliferation of H1299 (36).

ATRA loaded PCL-PEG-PCL nanomicelles caused significant cytotoxicity toward H1299 cells, and the IC_{50} of 10% and 2% feeding ratios were 50 µg/mL and higher than 200 µg/mL, respectively. In the case of free ATRA, no significant cytotoxicity was observed even for a concentration as much as 200 µg/mL.

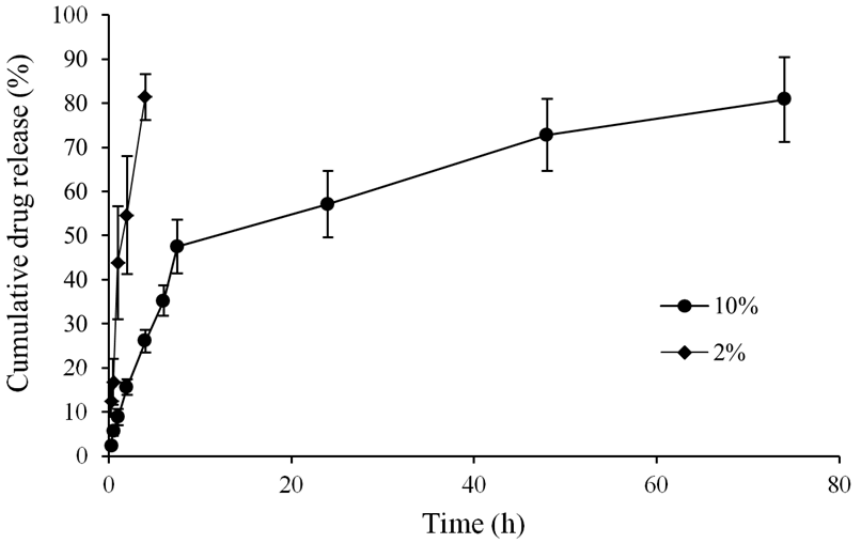

Fig. 6. ATRA cumulative release curve from PCL-PEG-PCL micelles for 96 h at 37 °C.

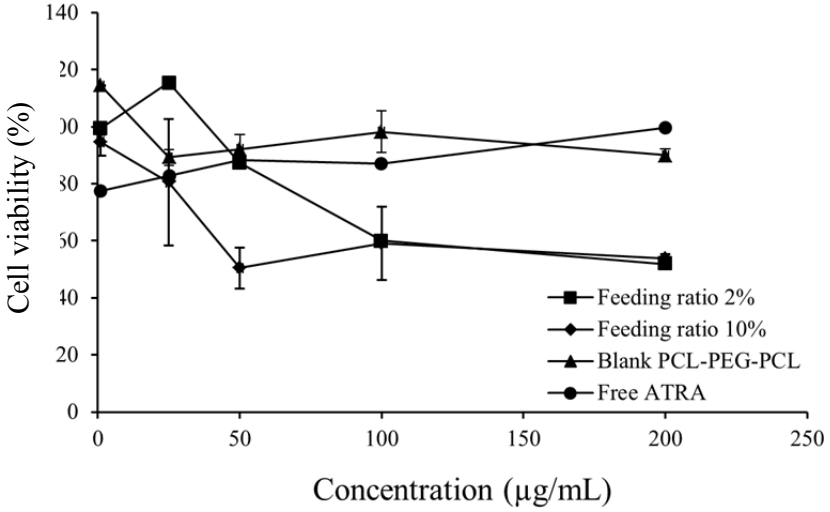

Fig. 7. Relative cell viability of PCL-PEG-PCL on H1299 cells.

DISCUSSION

In the present study, the PCL-PEG-PCL copolymer was synthesized successfully by the ring-opening copolymerization, and the synthesis was confirmed by ^{1}H NMR and FTIR spectra. The weight-average molecular weight was also measured by ^{1}H NMR spectrum and it was found in good agreement with the result measured by SLS technique (the weight average molecular weight measured by SLS technique was 5.34 ± 2.81 kDa and that measured by ^{1}H NMR spectrum was 5.26 kDa).

The CAC of the PCL-PEG-PCL micelles was determined using nile red. It could be expected for the micelles to be disassociated in the body fluids due to dilution of the micelle solutions in these fluids. The lower the CAC value, the more stable the micelles will be in the body fluids (37). The CAC of the PCL-PEG-PCL micelles was 1.9×10^{-3} g/L, which is around 1200 times lower than the required concentrations to form micelles with low molecular weight surfactants (e.g., sodium dodecyl sulfate with a CMC of 2.3 mg/mL) (37). The CAC value was also lower than that of PCL-PEG diblock copolymer micelles obtained by Jeong, (38), which was 0.0032 g/L.

The total fluorescence intensity varied negligibly at the low concentrations of micelles (lower than CAC). At CAC concentration, the total fluorescence intensity increased logarithmically by increasing the concentration of PCL-PEG-PCL copolymer. According to the results, it is obviously possible to form PCL-PEG-PCL micelles, even in highly diluted solutions.

For further analysis of the micelles, their size and zeta potential were determined. The obtained micelles were found in good stability during the time, and no significant changes were found in the size of micelles during a specific period. Another factor for the stability of micelles is the zeta potential. The average zeta potential of the micelles was -15.06 ± 1.65 mV, which was in an acceptable range for stable particles. According to the above consideration, the stability of this colloidal system during the time could be expected.

The FTIR spectrum of drug-loaded nanomicelles indicated that there is no interaction between the polymer and the drug. The presence of crystalline peaks in the XRD spectrum of drug-loaded nanomicelles indicates that ATRA is present in the crystalline form in the PCL-PEG-PCL nanomicelles which could be attributed to the aggregation of ATRA inside the core of micelles and consequently drug crystals could form in the core of nanomicelles.

The size of nanomicelles after loading the drug was determined, and it was found that the particle size increased with increasing the DC, which could be related to the higher amount of drug in the core of micelles.

Zeta potential can significantly affect the stability of particles in nanocolloidal systems because of the possible electrostatic repulsion between the particles (39). Since PEG has a negative charge, the zeta potential of nanomicelles was negative (40). The ATRA-loaded micelles possess higher zeta potential, due to the negative charge of ATRA, and there was a direct relation between DC and zeta potential; the higher the DC, the higher the zeta potential was observed. Thereby, zeta potential was -30.03 ± 3.42 mV for drug to polymer ratio of 20%.

The morphology of obtained micelles was observed using AFM. The size of nanomicelles obtained by AFM was found bigger than that obtained by DLS. This discrepancy can be attributed to the sample condition; micelles are in colloidal disperse form for DLS analysis, whereas they have been flattened in AFM analysis. As a result of deposition on the substrate surface, the size of micelles gets bigger in the surface direction of nanoparticles. Another possible reason for this discrepancy could be due to higher aggregation rate of nanoparticles in the dry form.

Also, AFM images show that, in comparison with blank micelles, micelle size decreased for 2% drug to polymer ratio while increased for 10% drug to polymerratio which is another confirmation for obtained data by DLS. AFM images showed that ATRA has an important effect on the morphology of PCL-PEG-PCL nanomicelles.

The release profile of ATRA from nanomicelles with 2 and 10% ratios was compared and it was observed that the release rate of ATRA from micelles with 10% drug to poymer ratio is significantly slower than that from micelles with 2% ratio. This slow and prolonged release for ratio of 10% is attributable to the hydrophobic nature of ATRA as well as its crystallization inside the micelle's core confirmed by XRD studies (Fig. 4c) (12,35). The release of hydrophobic drugs occurs slowly at high concentrations of the drug, due to the more hydrophobic environment at these concentrations. On the other hand, DC is higher for the case with 10% ratio. At low DCs, ATRA might be relatively present as a molecular dispersion inside the nanomicelles (38), while the crystallization of drug could occur at high DCs. The crystallized drugs need longer time to dissolve in release medium, and the release from the micelles occur more slowly compared to molecular dispersion. The release medium cannot freely penetrate into the inner part (micelle core) due to their strong hydrophobic core and crystallized drug in the core. The release profile of 2% ratio showed a burst release which is related to the diffusion and desorption of drug located close to the micelle surface (41,42). For nanomicelles with a feeding ratio of 10%, the drug is retained inside the core due to the slow drug leakage, and consequently, the drug is released only when the micelles are taken up by tumoral cells, and the PCL-PEG-PCL molecules are enzymatically decomposed. As a result, the concentration of the drug in tumors increases due to enhanced permeability and retention (EPR) effect (19).

With regard to the results of cytotoxicity of nanomicelles, it could be well observed that ATRA-loaded nanomicelles showed much more cytotoxic activity toward H1299 cell line compared to free ATRA. Both ATRAloaded nanomicelles (drug to polymer ratios of 2% and 10%) achieved IC_{50}, but for the free ATRA, IC_{50} could not be achieved. These results indicated that the encapsulation of ATRA in the PCL-PEG-PCL micelles enhances the cytotoxicity of ATRA. Because blank nanomicelles exhibited no cytotoxic activity in the concentration similar to drug-loaded nanomicelles, the higher cytotoxicity of encapsulated ATRA could be attributed to the enhanced solubility of ATRA in the form of nanomicelle. On the other hand, uptake of free ATRA is limited with its low water solubility which caused inefficacy of free form of the drug at higher concentrations. Another possible reason for higher cytotoxicity of encapsulated ATRA could be slow release profile of ATRA from ATRA-loaded micelles. The drug to polymer ratio of 10% showed higher cytotoxic effect than that of 2% while the amount of ATRA in both mixtures was the same. It could be attributed to the higher drug content of 10% probably because the nanoparticles with high loading content have more potential to overcome the tumor drug resistance (43). In a similar study, Firestone, *et al*, showed direct correlation between loading content and cytotoxicity of doxorubicin .

CONCLUSION

The synthesis of PCL-PEG-PCL was successfully achieved and used to fabricate ATRA-loaded nanomicelles. The CAC values of obtained micelles was low enough (1.9×10^{-3} g/L) to conclude that the micelles are stable even in highly diluted solutions. Furthermore, the acceptable size and zeta potential of these micelles could re-confirm their stability and efficient cellular uptake. The drug-loaded nanomicells exhibited prolonged ATRA release profiles and significant inhibition of H1299 cell proliferation. In conclusion, PCL-PEG-PCL nanomicelles could be considered as a great candidate for ATRA nanoparticulate drug delivery system with potential application in cancer therapy.

ACKNOWLEDGEMENTS

The authors would like to acknowledge the Research Council of Kermanshah University of Medical Sciences (Grant number: 93452) for financial support of this work.

REFERENCES

1. Huang ME, Ye YC, Chen SR, Chai JR, Lu JX, Zhoa L, *et al*. Use of all-trans retinoic acid in the

treatment of acute promyelocyte leukemia. Blood. 1988;72(2):567-572.
2. Defer GL, Adle-Biassette H, Ricolfi F, Martin L, Authier FJ, Chomienne C, *et al*. All-trans retinoic acid in relapsing malignant gliomas: clinical and radiological stabilization associated with the appearance of intratumoral calcifications. J Neurooncol. 1997;34(2):169-177.
3. Nikbakht Dastjerdi M, Zamani S, Mardani M, Hashemi Beni B. All-trans retinoic acid and genistein induce cell apoptosis in OVCAR-3 cells by increasing the P14 tumor suppressor gene. Res Pharm Sci. 2016; 11(6):505-512.
4. Lübbert M, Müller-Tidow C, Hofmann WK, Koeffler HP. Advances in the treatment of acute myeloid leukemia: from chromosomal aberrations to biologically targeted therapy. J Cell Biochem. 2008;104(6):2059-2070.
5. Nervi C, Vollberg TM, George MD, Zelent A, Chambon P, Jetten AM. Expression of nuclear retinoic acid receptors in normal tracheobronchial cells and in lung carcinoma cells. Exp Cell Res. 1991;195(1):163-170.
6. Treat J, Friedland D, Luginbuhl W, Meehan L, Gorman G, Miller W Jr, *et al*. Phase II trial of all-trans retinoic acid in metastatic non-small cell lung cancer. Cancer Invest. 1996;14(5):415-420.
7. Rigas JR, Miller VA, Zhang ZF, Klimstra DS, Tong WP, Kris MG, *et al*. Metabolic phenotypes of retinoic acid and the risk of lung cancer. Cancer Res. 1996;56(12):2692-2696.
8. Arrieta O, González-De la Rosa CH, Aréchaga-Ocampo E, Villanueva-Rodríguez G, Cerón-Lizárraga TL, Martínez-Barrera L, *et al*. Randomized phase II trial of all-trans-retinoic acid with chemotherapy based on paclitaxel and cisplatin as first-line treatment in patients with advanced non–small-cell lung cancer. J Clin Oncol. 2010;28(21):3463-3471.
9. Quintero Barceinas RS, García-Regalado A, Aréchaga-Ocampo E, Villegas-Sepúlveda N, González-De la Rosa CH. All-trans retinoic acid induces proliferation, survival, and migration in A549 lung cancer cells by activating the ERK signaling pathway through a transcription-independent mechanism. BioMed Res Inter. 2015; Article ID 404368: 10 pages.
10. Choi EJ, Whang YM, Kim SJ, Kim HJ, Kim YH. Combinational treatment with retinoic acid derivatives in non-small cell lung carcinoma *in vitro*. J Korean Med Sci. 2007; Suppl:S52-60.
11. Fang J, Chen SJ, Tong JH, Wang ZG, Chen GQ, Chen Z. Treatment of acute promyelocytic leukemia with ATRA and As2O3: a model of molecular target-based cancer therapy. Cancer Biol Ther. 2002;1(6):614-620.
12. Kim DG, Choi C, Jeong YI, Jang MK, Nah JW, Kang SK, *et al*. All-trans retinoic acid-associated low molecular weight water-soluble chitosan nanoparticles based on ion complex. Macromol Res. 2006;14(1):66-72.
13. Coradini D. New chemical strategies for overcoming ATRA resistance in APL cells. Leuk Res. 2006;31(3):291-302.
14. Szuts EZ, Harosi FI. Solubility of retinoids in water. Arch Biochem Biophys. 1991;287(2):297-304.
15. Brisaert MG, Everaerts I, Plaizier-Vercammen JA. Chemical stability of tretinoin in dermatological preparations. Pharm Acta Helv.1995;70(2):161-166.
16. Ioele G, Cione E, Risoli A, Genchi G, Ragno G. Accelerated photostability study of tretinoin and isotretinoin in liposome formulations. Int J Pharm. 2005;293(1-2):251-260.
17. Kawakami S, Opanasopit P, Yokoyama M, Chansri N, Yamamoto T, Okano T, *et al*. Biodistribution characteristics of all-trans retinoic acid incorporated in liposomes and polymeric micelles following intravenous administration. J Pharm Sci. 2005;94(12):2606-2615.
18. Li Y, Qi XR, Maitani Y, Nagai T. PEG-PLA diblock copolymer micelle-like nanoparticles as all-trans-retinoic acid carrier: *in vitro* and *in vivo* characterizations. Nanotechnology. 2009;20(5):055106.
19. Fattahi A, Golozar MA, Varshosaz J, Sadeghi HM, Fathi M. Preparation and characterization of micelles of oligomeric chitosan linked to all-trans retinoic acid. Carb Pol. 2012;87(2):1176-1184.
20. Hwang SR, Lim SJ, Park JS, Kim CK. Phospholipid-based microemulsion formulation of all-trans-retinoic acid for parenteral administration. Int J Pharm. 2004;276(1-2):175-183.
21. Seo SJ, Kim SH, Sasagawa T, Choi YJ, Akaike T, Cho CS. Delivery of all trans-retinoic acid (RA) to hepatocyte cell line from RA/galactosyl α-cyclodextrin inclusion complex. Eur J Pharm Biopharm. 2004;58(3):681-687.
22. Kataoka K, Harada A, Nagasaki Y. Block copolymer micelles for drug delivery: design, characterization and biological significance. Adv Drug Deliv Rev. 2001;47(1):113-131.
23. Sajadi Tabassi SA, Khodaverdi E, Hadizadeh F, Rashid R. Preparation of hydrogels based on inclusion complexes of the triblock copolymer PCL-PEG-PCL with α-cyclodextrin (α-CD). Res Pharm Sci. 2012;7(5):S975.
24. Edlund U, Albertsson AC. Degradable polymer microspheres for controlled drug delivery. Degradable aliphatic polyesters. Advances in Polymer Science. V. 157. Springer Berlin Heidelberg; 2002. pp. 67-112.
25. Herold DA, Keil K, Bruns DE. Oxidation of polyethylene glycols by alcohol dehydrogenase. Biochem Pharmacol. 1989;38(1):73-76.
26. Danafar H, Rostamizadeh K, Davaran S, Hamidi M. Preparation and characterization of PLA-PEG-PLA tri-block copolymer polymersomes as a novel carrier for lisinopril. Res Pharm Sci. 2012;7(5):S398.
27. Gong C, Shi S, Dong P, Kan B, Gou M, Wang X, *et al*. Synthesis and characterization of PEG-PCL-PEG thermosensitive hydrogel. Int J Pharm. 2009;365 (1-2):89-99.
28. Lin WJ, Wang CL, Juang LW. Characterization and comparison of diblock and triblock amphiphilic

copolymers of poly (δ-valerolactone). J Appl Pol Sci. 2006;100(3):1836-1841.
29. Liu CB, Gong CY, Huang MJ, Wang JW, Pan YF, Zhang YD, *et al*. Thermoreversible gel-sol behavior of biodegradable PCL-PEG-PCL triblock copolymer in aqueous solutions. J Biomed Mater Res B Appl Biomater. 2008;84(1):165-175.
30. Ge H, Hu Y, Jiang X, Cheng D, Yuan Y, Bi H, *et al*. Preparation, characterization, and drug release behaviors of drug nimodipine-loaded poly(ε-caprolactone)-poly(ethylene oxide)-poly(ε-caprolactone) amphiphilic triblock copolymer micelles. J Pharm Sci. 2002;91(6):1463-1473.
31. Debye P. Light scattering in solutions. J Appl Phys. 1944;15(4):338-342.
32. Jin Y. Nanotechnology in pharmaceutical manufacturing. Pharm Sci Encycl. 2010;32:1-32.
33. Fattahi A, Petrini P, Munarin F, Shokoohinia Y, Golozar MA, Varshosaz J, *et al*. Polysaccharides derived from tragacanth as biocompatible polymers and gels. J Appl Pol Sci. 2013;129(4):2092-2102.
34. Zhang L, Chen Z, Wang H, Wu S, Zhao K, Sun H, *et al*. Preparation and evaluation of PCL-PEG-PCL polymeric nanoparticles for doxorubicin delivery against breast cancer. RSC Adv. 2016;6(60):54727-54737.
35. Na K, Park KH, Kim SW, Bae YH. Self-assembled hydrogel nanoparticles from curdlan derivatives: characterization, anti-cancer drug release and interaction with a hepatoma cell line (HepG2). J Control Release. 2000;69(2):225-236.
36. Sun SY, Yue P, Shroot B, Hong WK, Lotan R. Induction of apoptosis in human non-small cell lung carcinoma cells by the novel synthetic retinoid CD437. J Cell Physiol. 1997;173(2):279-284.
37. Bian F, Jia L, Yu W, Liu M. Self-assembled micelles of N-phthaloylchitosan-g-polyvinylpyrrolidone for drug delivery. Carb Polym. 2009;76(3):454-459.
38. Jeong YI, Kang MK, Sun HS, Kang SS, Kim HW, Moon KS, *et al*. All-trans-retinoic acid release from core-shell type nanoparticles of poly (ε-caprolactone)/poly (ethylene glycol) diblock copolymer. Int J Pharm. 2004;273(1-2):95-107.
39. Dong Y, Feng SS. Methoxy poly(ethylene glycol)-poly(lactide) (MPEG-PLA) nanoparticles for controlled delivery of anticancer drugs. Biomaterials. 2004;25(14):2843-2849.
40. Hayashi K, Nakamura M, Sakamoto W, Yogo T, Miki H, Ozaki S, *et al*. Superparamagnetic nanoparticle clusters for cancer theranostics combining magnetic resonance imaging and hyperthermia treatment. Theranostics. 2013;3(6):366-376.
41. MacEwan SR, Callahan DJ, Chilkoti A. Stimulus-responsive macromolecules and nanoparticles for cancer drug delivery. Nanomedicine (Lond). 2010;5(5):793-806.
42. Kumari A, Yadav SK, Yadav SC. Biodegradable polymeric nanoparticles based drug delivery systems. Colloids Surf B Biointerfaces. 2010;75(1):1-18.
43. Oh N, Park JH. Endocytosis and exocytosis of nanoparticles in mammalian cells. Int J Nanomedicine. 2014;9(Suppl 1):51-63.